

Journal Pre-proof

The novel potential therapeutic target PSMP/MSMP promotes acute kidney injury via CCR2

Zhanming Song, Weijian Yao, Xuekang Wang, Yaqian Mo, Zhongtian Liu, Qingqing Li, Lei Jiang, Hui Wang, Huiying He, Ning Li, Zhaohuai Zhang, Ping Lv, Yu Zhang, Li Yang, Ying Wang

PII: S1525-0016(24)00330-7

DOI: <https://doi.org/10.1016/j.ymthe.2024.05.028>

Reference: YMTHE 6445

To appear in: *Molecular Therapy*

Received Date: 21 November 2023

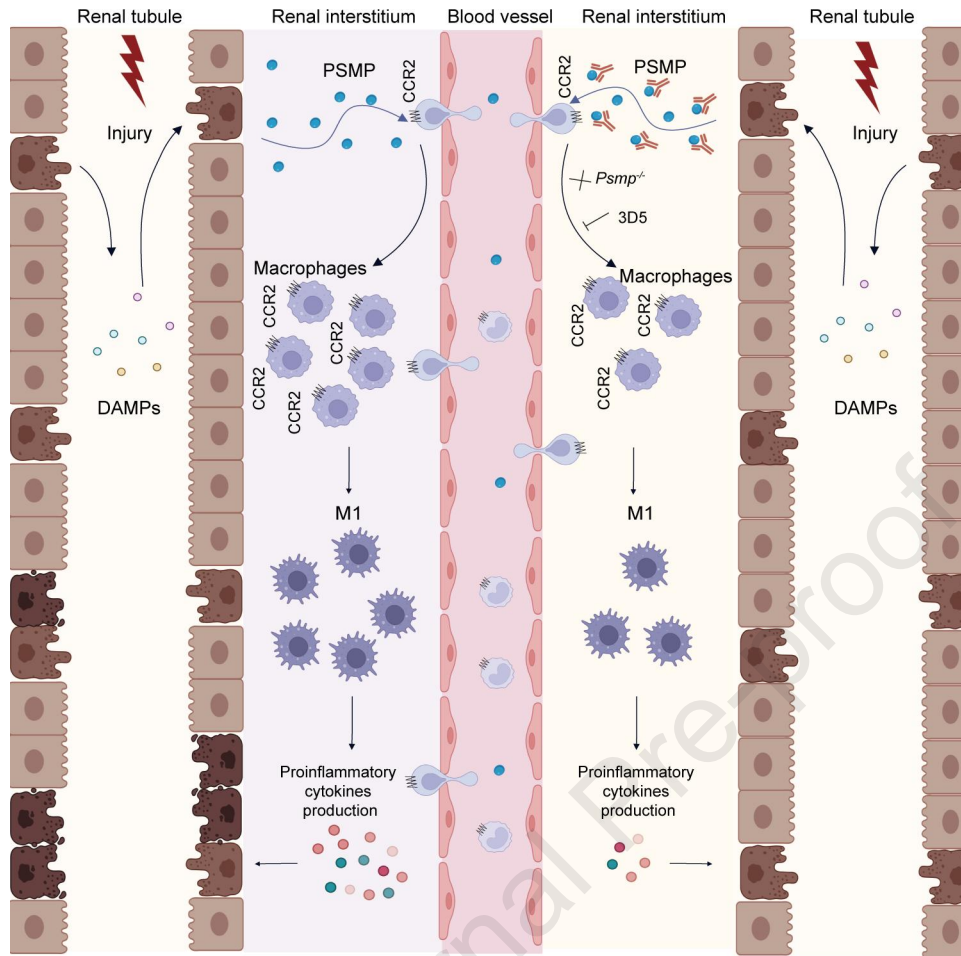
Accepted Date: 23 May 2024

Please cite this article as: Song Z, Yao W, Wang X, Mo Y, Liu Z, Li Q, Jiang L, Wang H, He H, Li N, Zhang Z, Lv P, Zhang Y, Yang L, Wang Y, The novel potential therapeutic target PSMP/MSMP promotes acute kidney injury via CCR2, *Molecular Therapy* (2024), doi: <https://doi.org/10.1016/j.ymthe.2024.05.028>.

This is a PDF file of an article that has undergone enhancements after acceptance, such as the addition of a cover page and metadata, and formatting for readability, but it is not yet the definitive version of record. This version will undergo additional copyediting, typesetting and review before it is published in its final form, but we are providing this version to give early visibility of the article. Please note that, during the production process, errors may be discovered which could affect the content, and all legal disclaimers that apply to the journal pertain.

© 2024





23 ABSTRACT

24 Acute kidney injury (AKI) is a major worldwide health concern that currently lacks effective
25 medical treatments. PSMP is a damage-induced chemotactic cytokine that acts as a ligand of CCR2
26 and has an unknown role in AKI. We have observed a significant increase in PSMP levels in the
27 renal tissue, urine, and plasma of patients with AKI. PSMP deficiency improved kidney function
28 and decreased tubular damage and inflammation in AKI mouse models induced by kidney
29 ischemia–reperfusion injury, glycerol, and cisplatin. Single-cell RNA sequencing analysis
30 revealed that Ly6C^{hi} or F4/80^{lo} infiltrated macrophages (IMs) were a major group of
31 proinflammatory macrophages with strong CCR2 expression in AKI. We observed that PSMP
32 deficiency decreased CCR2⁺Ly6C^{hi} or F4/80^{lo} IMs and inhibited M1 polarization in the AKI
33 mouse model. Moreover, overexpressed human PSMP in the mouse kidney, which could reverse
34 the attenuation of kidney injury in a CCR2-dependent manner, and this effect could be achieved
35 without CCL2 involvement. Extracellular PSMP played a crucial role, and treatment with a PSMP-
36 neutralizing antibody significantly reduced kidney injury *in vivo*. Therefore, PSMP might be a
37 therapeutic target for AKI, and its antibody is a promising therapeutic drug for the treatment of
38 AKI.

39 INTRODUCTION

40 Acute kidney injury (AKI) is a clinical complication characterized by sudden renal dysfunction
41 and is an increasing worldwide health concern.¹ AKI is associated with high morbidity, mortality,
42 and treatment costs.² Furthermore, AKI also increases the development of chronic kidney disease
43 (CKD) or end-stage renal disease and can even be life-threatening.^{3,4} Unfortunately, there are no
44 medications that can be used to stop kidney injury or promote kidney repair after injury.⁵

45 Inflammation is a complicated network of interactions between renal parenchymal cells and
46 immune cells that contributes to overall renal injury and is a primary pathogenic mechanism of
47 both AKI and CKD.⁶⁻⁸ Among the immune cell populations, macrophages play a crucial role in
48 the inflammatory response of AKI. Proinflammatory macrophages can amplify inflammation and
49 contribute to kidney injury by releasing proinflammatory cytokines and chemokines.⁹ Systemic
50 depletion of macrophages using liposomal clodronate has been shown to mitigate early kidney
51 injury in mice.¹⁰⁻¹² Targeting the recruitment and infiltration of macrophages represents a pivotal
52 therapeutic strategy for AKI.

53 PC3-secreted microprotein (PSMP) or microseminoprotein (MSMP) was first found in PC3 cells
54 and prostate cancer tissues and is expressed at low levels or not expressed in most normal
55 tissues.^{13,14} By screening candidate genes among human protein-coding genes in the human
56 genome using peripheral blood cell chemotaxis assays, the chemotactic activity of PSMP was first
57 discovered and identified.¹⁴ Our previous study showed that PSMP was highly expressed in
58 hepatocytes in human fibrotic/cirrhotic liver tissues, regardless of etiology, and exhibited low or
59 no expression in normal human liver tissues.¹⁵ PSMP is a damage-induced chemotactic cytokine.
60 The damage-associated molecule pattern (DAMP) molecules IL-33 and HMGB-1 can induce
61 mouse primary hepatocytes to produce PSMP.¹⁵ PSMP is a ligand of CCR2 that chemoattracts
62 peripheral blood monocytes and lymphocytes via CCR2, and the affinity of PSMP and CCR2 is
63 comparable to that of CCL2 and CCR2.¹⁴ The CCR2 signaling pathway has been demonstrated to
64 play an essential role in the recruitment of monocytes to inflammatory sites.^{10,16,17}

65 Several studies have demonstrated an association between PSMP and diseases characterized by
66 injury, inflammation or/and fibrosis. PSMP deficiency or blockade with a PSMP-neutralizing
67 antibody ameliorates hepatic fibrosis and DSS-induced colitis.^{15,18} A study showed that PSMP

68 expression was considerably increased in the kidney tissue of chronic active antibody-mediated
69 rejection (CAAMR) patients.¹⁹ In addition, PSMP expression correlated with macrophages in
70 CAAMR patients, and PSMP may be a histopathological diagnostic biomarker of CAAMR in
71 kidney transplantation.¹⁹ However, the role and function of PSMP in AKI are still unclear.

72 In this study, we characterized the role of PSMP in AKI patient samples and AKI mouse models.
73 We showed that PSMP expression was considerably increased in the renal tissue, urine, and plasma
74 of AKI patients. Then, we used PSMP-knockout mice and PSMP-neutralizing antibody to explore
75 the physiological and pathological functions of PSMP in AKI mouse models. The results
76 demonstrated that PSMP deficiency or blockade with a PSMP-neutralizing antibody improved
77 kidney function and decreased tubular damage and inflammation induced by bIRI, glycerol, or
78 cisplatin in mice. Overexpression of human PSMP (hPSMP) in the kidney demonstrated that
79 hPSMP mediated proinflammatory and injurious effects in a CCR2-dependent manner, and these
80 effects could be independent of CCL2 during the development of AKI. Mechanistically, our
81 analysis through published single-cell RNA sequencing (scRNA-seq) identified Ly6C^{hi} or F4/80^{lo}
82 infiltrated macrophages (IMs) as a primary proinflammatory macrophage population contributing
83 to kidney inflammation. PSMP deficiency decreased renal Ly6C^{hi} or F4/80^{lo} IMs infiltration and
84 inhibited M1 polarization in AKI. These results demonstrate that PSMP is a potential therapeutic
85 target for AKI.

86 RESULTS

87 **PSMP expression is upregulated in AKI patients and a mouse model**

88 To investigate the relationship between PSMP and AKI, we examined PSMP expression in kidney
89 biopsy samples obtained from AKI patients. The causes of AKI were defined as nephrotoxicity in

90 20 patients and ischemic injury in 7 patients. Serum creatinine levels at biopsy were
91 315.60 ± 273.10 $\mu\text{mol/l}$, and the peak serum creatinine level was 664.00 ± 446.00 $\mu\text{mol/l}$. Given the
92 limited case numbers for these conditions, we treated all AKI patients as a single cohort for
93 subsequent analyses. Immunohistochemical staining showed that renal PSMP expression was
94 significantly increased in AKI patients, whereas normal control kidney sections showed almost no
95 expression of PSMP (Figure 1A and B).

96 We then measured the levels of PSMP in the urine and plasma of AKI patients. The healthy control
97 group included 8 adults (50% male and 50.58 ± 19.04 years old). The level of PSMP in the urine of
98 healthy controls was 2.44 ± 1.87 ng/ml after correcting for creatinine, and the plasma level was
99 12.59 ± 6.63 ng/ml. The levels of PSMP in the urine and plasma samples of AKI patients were
100 significantly increased compared to those of healthy controls, as indicated by enzyme-linked
101 immunosorbent assay (ELISA) (Figure 1C and D). We found a positive correlation between urine
102 PSMP and KIM-1 (Figure 1E), suggesting an association between an increase in PSMP expression
103 and renal tubular damage. In addition, correlation analysis showed that urine PSMP levels were
104 positively associated with renal PSMP expression, but no significant correlation was found
105 between plasma PSMP levels and renal PSMP expression, suggesting that urine PSMP may be
106 excreted from kidney tissues (Figure 1F and G).

107 Renal PSMP expression was markedly increased in the early phase of the uIRI-induced AKI mouse
108 model (Figure 1H and I). TUNEL staining showed that PSMP was predominantly expressed in the
109 nonapoptotic region (Figure 1J). Furthermore, the increase in PSMP expression in the kidney was
110 localized to lotus tetragonolobus lectin (LTL, a brush border marker)-positive cells, as shown by
111 double immunofluorescence staining (Figure 1K). These results indicate that renal tubular
112 epithelial cells (TECs) produced PSMP during kidney injury.

113 **PSMP deficiency alleviates bIRI-induced AKI**

114 We established a bIRI-induced AKI mouse model in WT and PSMP-knockout (*Psm^{-/-}*) mice to
115 explore the functions of PSMP *in vivo*. Serum creatinine and BUN were significantly decreased in
116 *Psm^{-/-}* mice compared with WT mice, indicating improved kidney function (Figure 2A). Renal
117 mRNA expression levels of the tubular injury marker genes *Ngal* and *Kim-1* were decreased in
118 *Psm^{-/-}* mice (Figure 2B). PAS staining showed that *Psm^{-/-}* mice had significant reductions in
119 intratubular cast formation, debris, and loss of the brush border, suggesting the attenuation of
120 tubular damage (Figure 2C). Consistently, NGAL protein expression was notably decreased in
121 *Psm^{-/-}* mice, as measured by immunohistochemical staining and western blotting (Figure 2D and
122 E, Figure S14A). Furthermore, qPCR showed that renal mRNA expression levels of the
123 inflammatory cytokines *Ccl2*, *Il-1 β* , *Il-6*, and *Tnf- α* were reduced in *Psm^{-/-}* mice, indicating the
124 alleviation of inflammation (Figure 2F). Renal mRNA expression of *Ccr2* was significantly
125 decreased in *Psm^{-/-}* mice, suggesting that PSMP expression regulated the level of CCR2-positive
126 cells (Figure 2G). These results indicate that PSMP deficiency ameliorates bIRI-induced AKI.

127 **PSMP deficiency alleviates glycerol- and cisplatin-induced AKI**

128 To further investigate the role of PSMP in AKI due to other causes, we used mouse models induced
129 by glycerol and cisplatin. Following glycerol treatment, serum creatinine and BUN levels were
130 reduced in *Psm^{-/-}* mice (Figure S1A). NGAL and KIM-1 expression analysis and PAS staining
131 demonstrated that *Psm^{-/-}* mice had significantly reduced tubular damage (Figure S1B-E, Figure
132 S14B and C). We observed a decrease in the mRNA expression levels of the inflammatory
133 cytokines *Ccl2*, *Il-1 β* , *Il-6*, and *Tnf- α* in *Psm^{-/-}* mice (Figure S1F). Moreover, we also observed
134 that PSMP deficiency improved renal function, alleviated tubular damage, and decreased
135 inflammation in cisplatin-induced AKI (Figure S2, Figure S14D). Taken together, these results

136 suggest that PSMP promotes the occurrence and development of AKI induced by different causes.
137 **AAV9-hPSMP restores renal PSMP expression and promotes AKI in a CCR2-dependent**
138 **manner and may be independent of CCL2**

139 Our previous study showed that PSMP had 91.4% amino acid sequence homology between
140 humans and mice, and both human and mouse PSMP proteins chemoattract CCR2-expressing cells
141 *in vitro*.^{14,15,18} Therefore, we investigated whether the hPSMP protein affected AKI in mice using
142 AAV9. As expected, *Psmg*^{-/-} mice that received AAV9-hPSMP had increased hPSMP expression
143 in the kidney compared with those that received the control AAV9-null (Figure 3A, Figure S14E).
144 Four weeks after AAV9-hPSMP injection, we established a bIRI-induced AKI mouse model. We
145 found that hPSMP overexpression exacerbated kidney dysfunction, tubular damage, and
146 inflammation compared to the effects observed in *Psmg*^{-/-} mice injected with AAV9-null,
147 indicating that hPSMP could aggravate AKI (Figure 3B-F, Figure S3, Figure S14E). In addition,
148 renal mRNA expression of *Ccr2* was significantly increased after hPSMP overexpression (Figure
149 3G). We used PSMP- and CCR2-double-knockout (*Psmg*^{-/-}*Ccr2*^{-/-}) mice to evaluate whether CCR2
150 was essential for PSMP-mediated promotion AKI. The results showed that hPSMP
151 overexpression in *Psmg*^{-/-}*Ccr2*^{-/-} mice did not reverse the attenuation of AKI (Figure 3, Figure S3,
152 Figure S14E).

153 Previous studies^{20,21} and our work showed that AKI was accompanied by elevated levels of CCL2,
154 a classic CCR2 ligand. PSMP deficiency decreased the mRNA expression of CCL2 *in vivo* (Figure
155 2F). We investigated the impact of PSMP on the expression of CCL2 using WT bone marrow-
156 derived macrophages (BMDMs) *in vitro*. The results demonstrated a significant upregulation in
157 both mRNA and protein expression levels of CCL2 following PSMP stimulation of BMDMs
158 (Figure S4). Additionally, prior to PSMP stimulation, BMDMs were pretreated with the CCR2

159 antagonist RS504393, resulting in a reduction in the expression of CCL2, which indicated that
160 PSMP regulates the expression of CCL2 through CCR2 (Figure S4). Subsequently, we used
161 PSMP- and CCL2-double-knockout (*Psm^{-/-}Ccl2^{-/-}*) mice overexpressing hPSMP to explore
162 whether PSMP-mediated inflammation was dependent on CCL2. The results showed that hPSMP
163 overexpression in *Psm^{-/-}Ccl2^{-/-}* mice reversed the attenuation of AKI, indicating that PSMP could
164 promote bIRI-induced AKI independent of CCL2 (Figure S5).

165 **Neutralization of PSMP signaling alleviates AKI**

166 PSMP can be secreted from the cell, and markedly high expression of PSMP was detected in the
167 plasma of AKI patients (Figure 1D). Moreover, PSMP deficiency attenuated AKI induced by
168 different causes. Therefore, we explored whether secreted PSMP played a pivotal role in the
169 pathogenesis of AKI. The PSMP-neutralizing antibody 3D5 can recognize and specifically
170 neutralize PSMP *in vitro* and *in vivo*.^{14,15,18} We evaluated the effects of 3D5 administered via tail
171 vein injection before bIRI-induced AKI. As shown in Figure S6, 3D5 treatment decreased the
172 mortality rate of mice with bIRI (ischemia time: 30 min)-induced AKI. In bIRI (ischemia time: 20
173 min)-induced AKI, the 3D5 treatment group exhibited significantly lower serum creatinine and
174 BUN levels than the mIgG treatment group, indicating improved kidney function (Figure 4A). The
175 3D5 treatment group had decreased NGAL and KIM-1 expression and mitigated tubular damage,
176 as evidenced by qPCR, PAS staining, immunohistochemical staining, and western blotting (Figure
177 4B-E, Figure S14F). The qPCR results revealed that 3D5 markedly decreased the mRNA
178 expression levels of the inflammatory cytokines *Ccl2*, *Il-1 β* , *Il-6*, and *Tnf- α* (Figure 4F). In
179 addition, we also detected the mRNA expression level of *Ccr2*, which was decreased in the 3D5
180 treatment group (Figure 4G). We also investigated the protection effects of 3D5 in glycerol-
181 induced AKI. 3D5 treatment resulted in amelioration of kidney dysfunction, attenuation of tubular

182 injury, and reduction of inflammation (Figure S7, Figure S14G). These results showed that
183 blocking PSMP significantly ameliorated AKI induced by different etiologies, indicating that
184 secreted PSMP plays a crucial role in AKI, and 3D5 could be a promising treatment for AKI.

185 **Ly6C^{hi} or F4/80^{lo} infiltrated macrophages are proinflammatory macrophages in AKI**

186 To characterize the function of macrophage populations in the injured kidney, we further analyzed
187 published scRNA-seq data (GSE174324) of renal mononuclear phagocytic cell (MPC).²² Through
188 unsupervised clustering, these kidney MPCs were further classified into 15 macrophages based on
189 the typical monocyte/macrophage/dendritic cell markers and the comparison with the entire gene
190 expression based on Immunological Genome Project (ImmGen) mouse immune cell datasets. The
191 clusters C1-C4 were defined as kidney resident macrophages (KRM), while C6-C9 were defined
192 as Ly6C^{hi} IMs, and C12 was defined as Ly6C^{lo} IMs (Figure 5A, Figure S8, S9A, and Table S2).
193 By utilizing the differential genes of macrophages in peripheral blood, kidney, and spleen during
194 the steady-state period, and combining with previously published literature²², we constructed a
195 gene set specific to macrophages in three organs (see details in Table S3- “DEG of three organs at
196 NC” and “Organ gene set at NC”). Then we used this dataset to analyze the macrophages in the
197 kidneys during the acute phase of AKI, the results showed that the Ly6C^{hi} IMs in the kidney were
198 derived from peripheral blood and almost strongly expressed CCR2 (Figure 5B, C and E).
199 Compared to the other two clusters, Ly6C^{hi} IMs showed higher expression of inflammatory
200 cytokine, chemokine, and chemokine receptor (Figure 5G, Figure S9B).

201 In addition, we also characterized the features of F4/80^{lo} and F4/80^{hi} macrophages. We employed
202 the expression of *Adgre1* to define F4/80^{lo} and F4/80^{hi} macrophages. The clusters C1-C4 were
203 defined as F4/80^{hi} macrophages, and the clusters C6-C9 were identified as F4/80^{lo} macrophages
204 (Figure 5D, Figure S9A). Compared with F4/80^{hi} macrophages, F4/80^{lo} macrophages showed

205 higher expression of CCR2, inflammatory cytokine, chemokine, and chemokine receptor (Figure
206 5F, 5H, and Figure S9C).

207 Subsequently, we conducted an analysis of the Gene Ontology Biological Process (GOBP) of
208 Ly6C^{hi} IMs and F4/80^{lo} macrophages high expression genes and the key regulatory transcription
209 factors (TFs) of high expression genes (with TRRUST database) using Metascape (Figure S9D).
210 The data revealed that the high expression genes of Ly6C^{hi} IMs and F4/80^{lo} macrophages were
211 mainly enriched in inflammatory signaling pathways, such as “Neutrophil degradation”,
212 “Inflammatory response”, “Leukocyte migration”, etc. And the key regulatory transcription factors
213 included Nfkb1, Jun, and Cebpb. Additionally, we analyzed the protein protein interaction (PPI)
214 of Ly6C^{hi} IMs and F4/80^{lo} macrophages high expression genes in the STRING database (Figure
215 S9E). The data showed that the high expression genes of Ly6C^{hi} IMs and F4/80^{lo} macrophages
216 were mainly enriched in inflammatory signaling pathways, such as “Leukocyte migration”,
217 “Inflammatory response”, “Cell chemotaxis”, etc. These results indicate that Ly6C^{hi} or F4/80^{lo} IMs
218 are proinflammatory macrophages in AKI.

219 **PSMP deficiency inhibits renal proinflammatory macrophage infiltration**

220 We next investigated renal macrophages in WT and *Psmg*^{-/-} mice during bIRI- or uIRI-induced
221 AKI by flow cytometry (Figure S10). Compared with those in WT mice, renal CD11b^{hi}Ly6C^{hi} IMs
222 were significantly decreased in *Psmg*^{-/-} mice (Figure 6A and B; Figure S11A and B). We compared
223 CCR2⁺Ly6C^{hi} IMs between WT and *Psmg*^{-/-} mice and found a significant reduction in
224 CCR2⁺Ly6C^{hi} IMs in *Psmg*^{-/-} mice (Figure 6C and D; Figure S11C and D). Macrophages can be
225 identified into two subsets based on the fluorescence intensity of F4/80 and CD11b:
226 CD11b^{hi}F4/80^{lo} IMs and CD11b^{lo}F4/80^{hi} KRM.^{23,24} The data showed an increase in
227 CD11b^{hi}F4/80^{lo} IMs and a decrease in CD11b^{lo}F4/80^{hi} KRM in bIRI- or uIRI-induced AKI (Figure

228 6E and F; Figure S11E). CD11b^{hi}F4/80^{lo} IMs were significantly reduced in *Psmg*^{-/-} mice, while
229 CD11b^{lo}F4/80^{hi} KRM showed no differences compared with those in WT mice (Figure 6E and F;
230 Figure S11E).

231 In addition, we explored the impact of PSMP on macrophage infiltration in glycerol-induced AKI.
232 PSMP deficiency resulted in a decrease in both the proportion and population of CD11b^{hi}Ly6C^{hi}
233 IMs, CCR2⁺Ly6C^{hi} IMs and CD11b^{hi}F4/80^{lo} IMs compared to WT mice (Figure S12A-C). The
234 proportion of CD11b^{lo}F4/80^{hi} KRM was found to be increased in *Psmg*^{-/-} mice compared to WT
235 mice; however, no significant differences were observed within the population (Figure S12C).
236 Moreover, we also observed a significant reduction in CD11b^{hi}Ly6C^{hi} IMs, CCR2⁺Ly6C^{hi} IMs and
237 CD11b^{hi}F4/80^{lo} IMs in *Psmg*^{-/-} mice compared to WT mice following cisplatin-induced AKI
238 (Figure S13A-C), while no differences were found in CD11b^{lo}F4/80^{hi} KRM (Figure S13C).
239 Collectively, these findings indicate that PSMP exhibits a commonality mechanism in promoting
240 AKI induced by different causes, primarily by facilitating the infiltration of proinflammatory
241 macrophages.

242 **PSMP regulates macrophage phenotypic polarization**

243 We assessed the effect of PSMP on renal macrophage polarization *in vivo*. We used flow cytometry
244 to detect the polarization status of kidney F4/80⁺ macrophages in mice with bIRI-induced AKI
245 (Figure 7A). *Psmg*^{-/-} mice exhibited a noticeable reduction in the proportion of M1 and increase in
246 the proportion of M2 macrophages compared to WT mice (Figure 7 B). Moreover, we further
247 detected the polarization status of two subtypes of macrophages: CD11b^{hi}F4/80^{lo} IMs and
248 CD11b^{lo}F4/80^{hi} KRM (Figure 7C). PSMP deficiency significantly decreased the proportion of M1
249 macrophages and increased the proportion of M2 macrophages in CD11b^{hi}F4/80^{lo} IMs and
250 CD11b^{lo}F4/80^{hi} KRM (Figure 7D and E). In addition, we measured the mRNA levels of the M1

251 markers *Cd86*, *Nos2*, and *Il-12*, which were also significantly decreased in *Psmg^{-/-}* mice (Figure
252 7F).

253 DISCUSSION

254 Previously, we showed that PSMP is a damage-induced chemotactic cytokine that promotes the
255 progression of liver fibrosis in mouse models.¹⁵ Research has shown that PSMP expression is
256 increased in CAAMR and is correlated with macrophages.¹⁹ However, the function of PSMP in
257 AKI and the mechanism remain unknown. The aim of our current study was to clarify the role of
258 PSMP in AKI.

259 In this study, we examined PSMP expression in AKI patient samples. We found abundant
260 expression of PSMP in the biopsied kidney samples of AKI patients. Multiple timepoint analysis
261 showed a significant increase in PSMP protein expression during the early stage in the AKI mouse
262 model, and PSMP was predominantly expressed in the TUNEL-negative area of the injured
263 kidney. Further, through double immunofluorescence staining, we found that the increase in PSMP
264 was localized to TECs, indicating that TECs were producing PSMP. We hypothesized that the
265 expression of PSMP is regulated by the extracellular release of DAMPs in AKI, similar to liver
266 injury, which requires further investigation.

267 To explore the effects of the increase in PSMP on AKI, we used *Psmg^{-/-}* and WT mice to verify
268 that PSMP deficiency ameliorated kidney function and alleviated tubular damage and
269 inflammation in an AKI mouse model induced by bIRI, glycerol, and cisplatin compared with
270 those in WT mice. More importantly, overexpressing hPSMP in *Psmg^{-/-}* mice by using AAV9
271 vectors could reverse the attenuation of kidney injury, indicating that hPSMP could promote AKI.
272 AKI is accompanied by increased levels of CCL2.^{20,21} PSMP upregulated the expression of CCL2
273 in BMDMs *in vitro*. When genetic or pharmacological PSMP ablation occurred, the transcript

274 levels of CCL2 decreased *in vivo*. In addition, we investigated whether PSMP activity was CCL2-
275 dependent by overexpressing hPSMP in *Psmg^{-/-}Ccl2^{-/-}* mice via AAV9. The results indicated that
276 PSMP could promote bIRI-induced AKI without CCL2 involvement.

277 In further clinical sample detection, we performed a retrospective association study using urine
278 and plasma samples from AKI patients. We discovered significantly increased PSMP levels in the
279 urine and plasma of AKI patients, and urine PSMP levels were positively correlated with urine
280 levels of KIM-1, a tubular injury biomarker, suggesting that urine and plasma PSMP levels were
281 related to the pathological process of AKI. Moreover, we found that urine PSMP levels in AKI
282 patients were significantly associated with renal PSMP levels, while plasma PSMP levels showed
283 no significant correlation with renal PSMP levels. These findings suggest that urine PSMP
284 detection could be used to monitor kidney PSMP expression, providing a potential marker for
285 targeted PSMP therapy and a better understanding of the role and mechanism of PSMP in kidney
286 injury.

287 Previous reports have demonstrated that CCR2 deficiency ameliorates kidney injury and
288 inflammatory infiltration in the acute phase after IRI.^{17,25} Our previous study demonstrated that
289 PSMP was a ligand of CCR2.¹⁴ To determine whether CCR2 is required for PSMP-mediated
290 promotion of AKI, we overexpressed hPSMP in *Psmg^{-/-}* mice and *Psmg^{-/-}Ccr2^{-/-}* mice and
291 established a bIRI-induced AKI mouse model. However, the restoration of hPSMP expression in
292 *Psmg^{-/-}Ccr2^{-/-}* mice did not exacerbate kidney injury, as was observed in *Psmg^{-/-}* mice, indicating
293 that PSMP promoted AKI development in a CCR2-dependent manner.

294 The US Federal Drug Administration has not yet approved any drugs to treat or prevent AKI, and
295 most clinical care has been supportive and nonspecific.²⁶ We created the PSMP-specific
296 neutralizing antibody 3D5, which has significant antifibrotic effects on CCl₄-induced liver fibrosis

297 and anti-inflammatory effects on DSS-induced colitis.^{15,18} Here, we observed a significant
298 reduction in the mortality rate among bIRI (ischemia time: 30 min)-induced AKI mice following
299 3D5 treatment. 3D5 significantly improved renal function, mitigated tubular damage, and
300 attenuated inflammation mice with bIRI (ischemia time: 20 min)- or glycerol-induced AKI. These
301 results indicated that PSMP, which is a secreted protein, plays a crucial role in the pathogenesis of
302 AKI and could be a therapeutic target for AKI and that its antibody is a potential treatment option
303 for AKI.

304 It is well known that proinflammatory macrophages participate in inflammation during AKI.¹⁰
305 scRNA-seq provides accurate information on the complete gene structure and spatiotemporal
306 expression patterns of individual cells, enabling the identification of cellular heterogeneity and
307 functional annotation. To explore the mechanism by which PSMP affects AKI, we analyzed
308 published scRNA-seq data from the AKI acute phase.²² The analysis revealed that Ly6C^{hi} or
309 F4/80^{lo} IMs constituted major subsets of proinflammatory macrophages and that CCR2 was the
310 main receptor mediating renal injury. These findings provide support for previous studies that have
311 classified renal macrophages into distinct subsets based on the expression of Ly6C as Ly6C^{hi} and
312 Ly6C^{lo} subsets,²⁷ as well as based on the expression of F4/80 as F4/80^{lo} IMs and F4/80^{hi} KRM
313 subsets.^{24,25} We used *Psmpl*^{-/-} and WT mice to identify PSMP-mediated effects on macrophages.
314 During AKI induced by different etiologies, PSMP deficiency decreased CCR2⁺Ly6C^{hi} IMs or
315 F4/80^{lo} IMs infiltration.

316 Macrophages are a heterogeneous population, and the two main phenotypes, M1 and M2, play
317 diverse roles in mediating kidney injury and inflammation. Studies have proven that macrophages
318 can be polarized to the M1 phenotype in the early phase of kidney injury and actively participate
319 in the inflammatory response *in vitro* and in animal models.²⁸⁻³¹ M2 macrophages play a critical

320 role in resolving inflammation, promoting tissue remodeling, and facilitating recovery from AKI.³¹
321 Our previous study showed that PSMP regulated macrophage phenotype polarization *in vivo* and
322 *in vitro*.¹⁸ Consistently, this study showed that PSMP deficiency inhibited M1 polarization while
323 promoting M2 polarization. Overall, PSMP deficiency improved kidney injury by reducing
324 proinflammatory macrophage infiltration and inhibiting M1 polarization.

325 In conclusion, our study demonstrated the vital role of PSMP in AKI. PSMP is expressed at low
326 levels or not expressed in most normal tissues. We provided several lines of evidence showing that
327 PSMP was extensively and highly expressed in AKI patients. The upregulation of PSMP, which
328 is an upstream molecule associated with inflammatory pathogenesis, contributes to AKI in a
329 CCR2-dependent manner, and the effect may be independent of CCL2. PSMP deficiency
330 decreased proinflammatory macrophage infiltration and inhibited M1 polarization to alleviate
331 AKI. A PSMP antibody reduced kidney injury *in vivo*. These findings indicate that PSMP may be
332 a druggable target and that its antibody may be a promising therapeutic drug for AKI.

333 MATERIALS AND METHODS

334 **AKI patient samples**

335 AKI patients were from renal biopsy-AKI cross-sectional cohort during the years 2006-July 2020
336 in the Renal Division of Peking University First Hospital.²² Briefly, hospitalized AKI patients with
337 a pathological diagnosis of acute tubular injury on renal biopsy were included. The plasma and
338 urine samples of AKI patients were collected on the day of renal biopsy. The clinical characteristics
339 of the enrolled AKI patients were described in the previous study.²² Normal control kidney tissues
340 were from adjacent to renal cancer tissues ($n=9$). The protocol concerning the use of patient
341 samples in this study was approved by the Biomedical Research Ethics Committee of Peking

342 University First Hospital (approval number: 2023[373]). All enrolled participants provided written
343 informed consent.

344 **Human PSMP quantification**

345 The PSMP expression in the biopsied kidney samples of AKI patients was detected by
346 immunohistochemical staining. Kidney samples were fixed in 10% neutral buffered formalin
347 (Leagene) and paraffin-embedded kidney sections (4 μm). The kidney sections were
348 deparaffinized in dimethylbenzene and hydrated in 100%I, 100%II, 95%, and 75% ethanol, and
349 then placed in 1 \times phosphate-buffered saline (PBS). The prepared kidney sections used a high-
350 pressure method to expose antigens and 3% H_2O_2 for 20 min to remove peroxidase. The sections
351 were blocked with goat serum or 3% BSA for 40 min, then incubated with primary antibody,
352 mouse anti-PSMP monoclonal antibody (mAb) (3D5) at 4°C overnight. Secondary antibodies
353 (ZSGB-BIO, China) were applied and detected with a DAB kit (ZSGB-BIO, China).
354 Subsequently, sections were briefly counterstained with hematoxylin and mounted with neutral
355 gum. The normal control was from renal tissue adjacent to renal tumors.

356 Midstream samples of first voided morning urine and blood were collected from patients on the
357 day of renal biopsy. All urine and blood samples in this study were approved by the Biomedical
358 Research Ethics Committee of Peking University First Hospital (approval number: 2023[373]).
359 All enrolled participants provided written informed consent. Morning urine samples from 8 healthy
360 volunteers with informed consent were collected as healthy controls. Blood samples of 36 healthy
361 donors with informed consent were used as healthy controls. These volunteers were from the
362 Health Examination Center of Peking University First Hospital with normal urinalysis and blood
363 tests and had been excluded for chronic diseases such as hypertension, cardiovascular diseases,
364 diabetes, systemic diseases, etc. All blood and urine samples were centrifuged, and plasma and

365 urine supernatant were collected and stored at -80°C . The PSMP levels in the urine and plasma
366 were measured with the human MSMP/Prostate-associated microseminoprotein ELISA Kit
367 (EK21027, SAB) following the manufactural protocol.

368 **Animals**

369 Our previous study described the generation of wild-type (WT), *Psm^{-/-}*, *Psm^{-/-}Ccr2^{-/-}* mice.¹⁵ The
370 CCL2 knockout (*Ccl2^{-/-}*) mice on a C57BL/6 background were purchased from the Jackson
371 Laboratory (Bar Harbour, USA). PSMP- and CCL2-double-knockout mice (*Psm^{-/-}Ccl2^{-/-}*) were
372 generated by crossing *Psm^{-/-}* mice with *Ccl2^{-/-}* mice. Mice were housed and bred under specific-
373 pathogen-free facility at the Peking University Health Science Center or Peking University First
374 Hospital Animal Center. All experiments were conducted following the Guidelines for the Care
375 and Use of Laboratory Animals and with the approval of the Ethics Committee of Peking
376 University Health Science Center (PUIRB-LA2023285) or Peking University First Hospital
377 Animal Center (J202134).

378 **bIRI /unilateral IRI (uIRI) mouse models**

379 Kidney ischemia-reperfusion injury surgery was performed as previously reported.³² Male mice
380 (25~27 g) were anesthetized by intraperitoneal injection of 2.5% avertin (15 ml/kg). The mouse
381 body temperature was maintained at 37°C during the whole surgery with a temperature-controlled
382 machine. For bIRI, both kidneys were exposed, and the renal pedicles were clamped for 30 min.
383 In the sham group, only anesthesia and muscle incision were performed. The mice were sacrificed
384 24 h after surgery. For uIRI, the left back skin was cut open, and the left kidney was exposed. The
385 renal pedicle was carefully dissected and clamped with a vascular clip for 45 min. The mice were
386 sacrificed 0 h, 2 h, 6 h, 12 h, 24 h after surgery.

387 Other mouse models

388 For glycerol-induced AKI, male mice (28~30 g) were intramuscularly injected in each thigh caudal
389 muscle with 50% glycerol (7.5 ml/kg body weight) (Solarbio, China) or vehicle. The mice were
390 sacrificed 48 h after glycerol injection. For cisplatin-induced AKI, male mice (~25 g) were
391 intraperitoneally injected with cisplatin (20 mg/kg body weight) (Sigma Aldrich, USA) or vehicle.
392 The mice were sacrificed 72 h after cisplatin injection.

393 Mouse serum creatinine and blood urea nitrogen (BUN) quantification

394 Serum was collected from fresh mouse blood after centrifugation at 4500 rpm for 10 min. Serum
395 creatinine and BUN were measured by assay kits following the manufactural protocols (Nanjing
396 Jiancheng Bioengineering Institute, China).

397 Reverse transcription PCR and quantitative PCR (qPCR)

398 Total RNA was extracted and purified from frozen mouse kidney tissues using TRIzol Reagent
399 (Life Technologies, USA). Equal RNA (2 µg) was detected using nanodrop photometric
400 quantification (Thermo Scientific, USA), and then RNA was reverse-transcribed to cDNA using
401 Hifair II 1st Strand cDNA Synthesis SuperMix (Yeasen Biotech, China). Real-time qPCR was
402 performed with Hieff qPCR SYBR Green Master Mix (Yeasen Biotech, China) on an Mx3000P
403 Real-Time PCR System (Agilent Technologies, USA), and the PCR program included 95°C for
404 10 min; 40 cycles of 95°C for 15 s, 60°C for 60 s, and 72°C for 30 s; 95°C for 30 s, 55°C for 30 s,
405 and 95°C for 30 s. All gene expression levels were normalized to that of *Gapdh*. The primers used
406 in this study are shown in Table S1.

407 Kidney histological analyses, immunohistochemistry, and immunofluorescence

408 Kidney samples were fixed in 4% neutral paraformaldehyde solution, dehydrated in 70%, 80%,
409 95%, 100% I, 100% II ethanol and dimethyl benzene, subsequently embedded in paraffin and cut
410 into 4 μ m sections. The sections were deparaffinized in dimethylbenzene and hydrated in 100% I,
411 100% II, 95%, and 75% ethanol, and then placed in 1 \times PBS.

412 For PAS staining, the prepared kidney sections were stained with PAS staining kit following the
413 manufactural protocol (Solarbio, China). The degree of renal tubular acute injury was assessed by
414 two renal pathologists blinded to the experimental groups. The scores were based on a 0 to 4+
415 scale, according to the percentage of the cortex and medullar junction region affected by the loss
416 of renal tubular epithelial cells brush border, tubular necrosis and/or apoptosis, tubular cast,
417 interstitial inflammation (0 = no lesion, 1+ = < 25%, 2+ = > 25 to 50%, 3+ = > 50 to 75%, 4+ = >
418 75 to < 100%). The sum of each score was employed to derive the ultimate tubular injury score.

419 For immunohistochemistry, the prepared kidney sections used a high-pressure method to expose
420 antigens and 3% H₂O₂ for 20 min to remove peroxidase. The sections were blocked with goat
421 serum or 3% BSA for 40 min, then incubated with primary antibody, anti-rabbit PSMP pAb or
422 anti-goat NGAL pAb (AF1857, R&D Systems, USA) at 4°C overnight. Secondary antibodies
423 (ZSGB-BIO, China) were applied and detected with a DAB kit (ZSGB-BIO, China).
424 Subsequently, sections were briefly counterstained with hematoxylin and mounted with neutral
425 gum.

426 For immunofluorescence, the prepared kidney sections used a high-pressure method to expose
427 antigens, and 3% H₂O₂ to remove peroxidase. Primary antibody anti- rabbit PSMP pAb and LTL
428 were incubated in the sections at 4°C overnight. Then, avidin-FITC was incubated in the sections
429 at 4°C overnight. Goat anti-rabbit conjugated with Alexa Fluor 594 (ZSGB-Bio, China) was
430 utilized as secondary antibodies for 1 h at room temperature. The sections were dyed nucleus with

431 DAPI (Sigma, USA) for 5 min at room temperature. Slices were mounted with Fluorescence
432 Mounting Medium (Dako, Denmark) and imaged by BZ-X800.

433 **Terminal deoxynucleotidyl transferase-mediated deoxyuridine triphosphate nick end** 434 **labeling (TUNEL) assay**

435 Kidney TUNEL staining was performed using the TUNEL Apoptosis Detection Kit (Alexa Fluor
436 488, Yeasen Biotech, China) following the manufactural protocol.

437 **Western blot analysis**

438 The samples were subjected to 15% SDS PAGE electrophoresis and transferred to PVDF
439 membranes (Millipore Corporation, USA). The membrane was blocked with 5% BSA in TBST
440 for 1 h at room temperature and subsequently incubated with primary antibody, anti-rabbit PSMP
441 pAb or anti-goat NGAL pAb (AF1857, R&D Systems, USA) at 4°C overnight. Next, the
442 membrane was incubated with IRDye 800CW donkey anti-mouse IgG, IRDye 680LT donkey anti-
443 rabbit IgG, and IRDye 680LT donkey anti-goat IgG secondary Ab (LI-COR, USA) at room
444 temperature for 1 h in the dark. Finally, the fluorescence intensity was detected on membranes
445 with the LI-COR Infrared Imaging System and analyzed using Odyssey software.

446 **Single-cell RNA sequencing data analysis**

447 scRNA-seq data were processed as described in the published study.²²

448 **Flow cytometry**

449 The kidney was cut into small fragments and incubated for 30 min at 37°C with gentle shaking in
450 lysis solution: HBSS with 4 µg/µl collagenase type IV (Solarbio, China) and 0.5 µg/µl DNase I
451 (Sigma-Aldrich, USA). After enzymatic digestion, cells were passed through a 70 µm nylon mesh
452 filter and centrifuged at 2000 rpm at 4°C for 5 min to remove fragments. Then, the cell pellet was

453 suspended in 30% Percoll to acquire immune cells. Next, the pellet was incubated with ACK
454 Lysing Buffer for 3 min on ice and ended with cold PBS to remove red blood cells. The prepared
455 cells were incubated on ice with the Fc blocker (BD Biosciences, USA) for 10 min and then
456 incubated in the dark with fluorescence-labeled antibodies for 30 min.

457 The antibodies used in this study included anti-mouse CD45-FITC (103108), anti-mouse CD11b-
458 APC-Cy7 (101226), anti-mouse F4/80-PE (123109), anti-mouse F4/80-Percp-Cy5.5 (123127),
459 anti-mouse Ly6G-PE-Cyanine7 (127616), anti-mouse Ly6C-APC (128016), anti-mouse CD206
460 (141705), and anti-mouse I-A/I-E (MHCII, 107613), which were purchased from BioLegend (San
461 Diego, USA) and anti-mouse CCR2-PE (FAB5538P, R&D, USA). The cells were resuspended
462 after unbound antibodies were removed, then cells were acquired by BD FACS Verse (BD
463 Biosciences, USA). Data were analyzed by FlowJo software (FlowJoV10.0, TreeStar, Ashland,
464 OR, USA).

465 **AAV9-hPSMP construction and injection**

466 The AAV9 delivery system that overexpresses the hPSMP gene in mouse kidneys was constructed
467 by Vigene Bioscience (Shangdong, China). The empty associated adenovirus (AAV9-null) served
468 as a control. Titers of the vector genome were measured by quantitative reverse-transcription PCR
469 (qPCR) with vector-specific primers. Four-week-old male *Psm^{-/-}* mice, *Psm^{-/-}Ccr2^{-/-}* mice, and
470 *Psm^{-/-}Ccl2^{-/-}* mice were tail vein injected with AAV9-hPSMP (1×10^{12} v.g./mice) or AAV9-null
471 for 4 weeks before bIRI (ischemia time: 30 min)-induced AKI. The mice were sacrificed 24 h after
472 surgery.

473 **Mouse bone marrow-derived macrophages culture and treatment**

474 The bone marrow cells were flushed from tibias and femurs of 8-week-old male WT mice. Red
475 blood cells were removed by Red Blood Cell Lysis Buffer. After being washed, the cell suspension
476 was passed through a 40 μm cell strainer and then plated in a 6-well plate at a density of 2×10^6
477 cells per well. The medium used for culturing the BMDMs consisted of high-glucose Dulbecco's
478 modified Eagle's medium (DMEM) supplemented with 10% fetal bovine serum (FBS), 100
479 mg/mL streptomycin (PS), and 20 ng/mL macrophage colony-stimulating factor (M-CSF,
480 ProteinTech, USA). The BMDMs were incubated under these conditions for 7 days and the culture
481 medium was replaced every 3 days. To investigate the effect of PSMP on CCL2 expression,
482 BMDMs were treatment with either fresh culture medium (as a control), or PSMP (300 ng/ml), or
483 lipopolysaccharide (LPS, 100 ng/ml, Sigma-Aldrich, USA), or PSMP (300 ng/ml) + LPS (100
484 ng/ml), or pretreated with 3 μM RS 504393 (CCR2 antagonist, Sigma-Aldrich, USA) for 30 min.
485 The cells were collected at 4 h for qPCR and the cellular supernatants were collected at 24 h for
486 CBA.

487 **Cytometric bead assay (CBA)**

488 The CCL2 protein levels in cellular supernatants were quantified using a customized
489 LEGENDplexTM mouse inflammation panel (BioLegend, USA) following the manufacturer's
490 instructions. The data were acquired using a BD FACS Verse (BD Biosciences, USA) and
491 analyzed with official online analysis software (<https://legendplex.qognit.com>). The concentration
492 of CCL2 was determined by means of a standard curve generated during the performance of the
493 assay.

494 **The preparation of rabbit anti-PSMP polyclonal antibody (pAb) and mouse anti-PSMP mAb** 495 **(3D5)**

496 Rabbits and mice were immunized using the PSMP prokaryotic protein. The pAbs were purified
497 from rabbit serum by PSMP peptide coupled to Sepharose 4B. The monoclonal hybridoma cell
498 lines to PSMP were injected into the mouse abdominal cavity, and ascites were obtained. The
499 mAbs were purified by protein-G.

500 **Antibody treatments**

501 Six-week-old male WT mice were tail vein injected with 10 mg/kg 3D5 or mIgG for 24 h before
502 bIRI (ischemia time: 30min or 20 min)-induced AKI. The mice were sacrificed 24 h after surgery.

503 **Statistical analysis**

504 Statistical analysis was performed using GraphPad Prism 8.0.2 software (GraphPad Software,
505 USA). Sample exclusion was performed for data analyses based on identifying outliers (ROUT
506 method) of GraphPad Prism software. Differences between the two groups were compared using
507 Student's *t* test. Differences between multiple groups were determined using ordinary one-way
508 ANOVA with Dunnett's multiple comparisons test or Tukey's multiple comparisons test, and two-
509 way ANOVA with Sidak's multiple comparisons test. Pearson correlation analysis was used to
510 assess the correlation between two variables. Comparison of Survival Curves was determined by
511 Log-rank (Mantel-Cox) test. All data are expressed as the mean \pm standard error of the mean
512 (SEM), $P < 0.05$ was considered statistically significant.

513 **DATA AND CODE AVAILABILITY**

514 The scRNA-seq data used in this study have been deposited in the National Center for
515 Biotechnology Information Gene Expression Omnibus (GSE174324) and can be accessed at
516 <https://ncbi.nlm.nih.gov/geo/query/acc.cgi?acc=GSE174324>.

517 **KEYWORDS**

518 Acute kidney injury; Anti-PSMP antibody; CCR2; Macrophages; inflammation

519 ACKNOWLEDGMENTS

520 We are grateful to Professor Dalong Ma (Department of Immunology, School of Basic Medical
521 Sciences, NHC Key Laboratory of Medical Immunology and Center for Human Disease
522 Genomics, Peking University) for initiating functional genomics research and valuable
523 suggestions. We thank Professor Wenjie Hu (Department of Periodontology, Peking University
524 School and Hospital of Stomatology) and Dr. Wenting Jiang (Department of Periodontology,
525 Peking University School and Hospital of Stomatology) for the cooperation.

526 This work was supported by the Natural Science Foundation of Beijing Municipality (7232089 to
527 Ying Wang), the National Natural Science Foundation of China (82271884 to Ying Wang and
528 81970536 to Ying Wang), the Open Fund of National Health Commission Key Laboratory of
529 Medical Immunology (Peking University) 2021KF06 (The funding is partially allocated to Ying
530 Wang), and the National Natural Science Foundation of China (82300759 to Weijian Yao). The
531 Graphical Abstracts created with BioRender.com.

532 AUTHOR CONTRIBUTIONS

533 Y.W., L.Y., Z.M.S., and W.J.Y. conceived the project, designed the experiments. Z.M.S.
534 performed most of the experiments and analysis. W.J.Y performed clinical samples collection and
535 analysis, and scRNA-seq analysis. X.K.W., Y.Q.M., Z.T.L., Q.Q.L., H.Y.H., N.L., Z.H.Z., P.L.,
536 and Y.Z. contributed to some experiments. L.J. and H.W. assessed tissue histology. Z.M.S. and
537 W.J.Y. drafted the manuscript. Y.W. and L.Y. reviewed and edited the manuscript. All authors
538 have read, verified, and approved this manuscript.

539 DECLARATION OF INTERESTS

540 Y.W., Z.M.S., Z.T.L., and Q.Q.L. are co-inventors on a patent covering PSMP antagonists for use
541 in treatment of diseases.

542 REFERENCES

- 543 1. Lameire, N.H., Bagga, A., Cruz, D., De Maeseneer, J., Endre, Z., Kellum, J.A., Liu, K.D.,
544 Mehta, R.L., Pannu, N., Van Biesen, W., et al. (2013). Acute kidney injury: an increasing
545 global concern. *Lancet* (London, England) 382, 170-179.
- 546 2. Hoste, E.A.J., Kellum, J.A., Selby, N.M., Zarbock, A., Palevsky, P.M., Bagshaw, S.M.,
547 Goldstein, S.L., Cerda, J., and Chawla, L.S. (2018). Global epidemiology and outcomes of
548 acute kidney injury. *Nat Rev Nephrol* 14, 607-625.
- 549 3. See, E.J., Jayasinghe, K., Glassford, N., Bailey, M., Johnson, D.W., Polkinghorne, K.R.,
550 Toussaint, N.D., and Bellomo, R. (2019). Long-term risk of adverse outcomes after acute
551 kidney injury: a systematic review and meta-analysis of cohort studies using consensus
552 definitions of exposure. *Kidney Int* 95, 160-172.
- 553 4. Chawla, L.S., Eggers, P.W., Star, R.A., and Kimmel, P.L. (2014). Acute kidney injury and
554 chronic kidney disease as interconnected syndromes. *N Engl J Med* 371, 58-66.
- 555 5. de Caestecker, M., and Harris, R. (2018). Translating Knowledge Into Therapy for Acute
556 Kidney Injury. *Semin Nephrol* 38, 88-97.
- 557 6. Andrade-Oliveira, V., Foresto-Neto, O., Watanabe, I.K.M., Zatz, R., and Camara, N.O.S.
558 (2019). Inflammation in Renal Diseases: New and Old Players. *Front Pharmacol* 10, 1192.
- 559 7. Bonventre, J.V., and Zuk, A. (2004). Ischemic acute renal failure: an inflammatory disease?
560 *Kidney Int* 66, 480-485.
- 561 8. Han, S.J., and Lee, H.T. (2019). Mechanisms and therapeutic targets of ischemic acute
562 kidney injury. *Kidney Res Clin Pract* 38, 427-440.

- 563 9. Wen, Y., Yan, H.R., Wang, B., and Liu, B.C. (2021). Macrophage Heterogeneity in Kidney
564 Injury and Fibrosis. *Front Immunol* 12, 681748.
- 565 10. Cao, Q., Harris, D.C., and Wang, Y. (2015). Macrophages in kidney injury, inflammation,
566 and fibrosis. *Physiology (Bethesda)* 30, 183-194.
- 567 11. Okubo, K., Kurosawa, M., Kamiya, M., Urano, Y., Suzuki, A., Yamamoto, K., Hase, K.,
568 Homma, K., Sasaki, J., Miyauchi, H., et al. (2018). Macrophage extracellular trap formation
569 promoted by platelet activation is a key mediator of rhabdomyolysis-induced acute kidney
570 injury. *Nat Med* 24, 232-238.
- 571 12. Ferenbach, D.A., Sheldrake, T.A., Dhaliwal, K., Kipari, T.M.J., Marson, L.P., Kluth, D.C.,
572 and Hughes, J. (2012). Macrophage/monocyte depletion by clodronate, but not diphtheria
573 toxin, improves renal ischemia/reperfusion injury in mice. *Kidney Int* 82, 928-933.
- 574 13. Valtonen-Andre, C., Bjartell, A., Hellsten, R., Lilja, H., Harkonen, P., and Lundwall, A.
575 (2007). A highly conserved protein secreted by the prostate cancer cell line PC-3 is
576 expressed in benign and malignant prostate tissue. *Biol Chem* 388, 289-295.
- 577 14. Pei, X., Sun, Q., Zhang, Y., Wang, P., Peng, X., Guo, C., Xu, E., Zheng, Y., Mo, X., Ma, J.,
578 et al. (2014). PC3-secreted microprotein is a novel chemoattractant protein and functions as
579 a high-affinity ligand for CC chemokine receptor 2. *J Immunol* 192, 1878-1886.
- 580 15. She, S., Wu, X., Zheng, D., Pei, X., Ma, J., Sun, Y., Zhou, J., Nong, L., Guo, C., Lv, P., et
581 al. (2020). PSMP/MSMP promotes hepatic fibrosis through CCR2 and represents a novel
582 therapeutic target. *J Hepatol* 72, 506-518.
- 583 16. Braga, T.T., Correa-Costa, M., Silva, R.C., Cruz, M.C., Hiyane, M.I., da Silva, J.S., Perez,
584 K.R., Cuccovia, I.M., and Camara, N.O.S. (2018). CCR2 contributes to the recruitment of

- 585 monocytes and leads to kidney inflammation and fibrosis development.
- 586 *Inflammopharmacology* 26, 403-411.
- 587 17. Furuichi, K., Wada, T., Iwata, Y., Kitagawa, K., Kobayashi, K.-I., Hashimoto, H., Ishiwata,
588 Y., Asano, M., Wang, H., Matsushima, K., et al. (2003). CCR2 signaling contributes to
589 ischemia-reperfusion injury in kidney. *J Am Soc Nephrol* 14, 2503-2515.
- 590 18. Pei, X., Zheng, D., She, S., Ma, J., Guo, C., Mo, X., Zhang, Y., Song, Q., Zhang, Y., Ma, D.,
591 et al. (2017). The PSMP-CCR2 interactions trigger monocyte/macrophage-dependent colitis.
592 *Sci Rep* 7, 5107.
- 593 19. Zhan, P., Li, H., Han, M., Wang, Z., Zhao, J., Tu, J., Shi, X., and Fu, Y. (2021). PSMP Is
594 Discriminative for Chronic Active Antibody-Mediated Rejection and Associate With Intimal
595 Arteritis in Kidney Transplantation. *Front Immunol* 12, 661911.
- 596 20. Jia, P., Xu, S., Ren, T., Pan, T., Wang, X., Zhang, Y., Zou, Z., Guo, M., Zeng, Q., Shen, B.,
597 et al. (2022). LncRNA IRAR regulates chemokines production in tubular epithelial cells thus
598 promoting kidney ischemia-reperfusion injury. *Cell Death Dis.* 13, 562.
- 599 21. Munshi, R., Johnson, A., Siew, E.D., Ikizler, T.A., Ware, L.B., Wurfel, M.M., Himmelfarb,
600 J., and Zager, R.A. (2011). MCP-1 gene activation marks acute kidney injury. *J Am Soc*
601 *Nephrol* 22, 165-175.
- 602 22. Yao, W., Chen, Y., Li, Z., Ji, J., You, A., Jin, S., Ma, Y., Zhao, Y., Wang, J., Qu, L., et al.
603 (2022). Single Cell RNA Sequencing Identifies a Unique Inflammatory Macrophage Subset
604 as a Druggable Target for Alleviating Acute Kidney Injury. *Adv Sci (Weinh)* 9, e2103675.
- 605 23. Belliere, J., Casemayou, A., Ducasse, L., Zakaroff-Girard, A., Martins, F., Iacovoni, J.S.,
606 Guilbeau-Frugier, C., Buffin-Meyer, B., Pipy, B., Chauveau, D., et al. (2015). Specific

- 607 macrophage subtypes influence the progression of rhabdomyolysis-induced kidney injury. *J*
608 *Am Soc Nephrol* 26, 1363-1377.
- 609 24. Huang, W., Wang, B., Hou, Y., Fu, Y., Cui, S., Zhu, J., Zhan, X., Li, R., Tang, W., Wu, J.,
610 et al. (2022). JAML promotes acute kidney injury mainly through a macrophage-dependent
611 mechanism. *JCI Insight* 7.
- 612 25. Li, L., Huang, L., Sung, S.-S.J., Vergis, A.L., Rosin, D.L., Rose, C.E., Lobo, P.I., and
613 Okusa, M.D. (2008). The chemokine receptors CCR2 and CX3CR1 mediate
614 monocyte/macrophage trafficking in kidney ischemia-reperfusion injury. *Kidney Int* 74,
615 1526-1537.
- 616 26. Hulse, M., and Rosner, M.H. (2019). Drugs in Development for Acute Kidney Injury. *Drugs*
617 79, 811-821.
- 618 27. Li, Y., Zhang, Y., Pan, G., Xiang, L., Luo, D., and Shao, J. (2022). Occurrences and
619 Functions of Ly6Chi and Ly6Clo Macrophages in Health and Disease. *Frontiers In*
620 *Immunology* 13, 901672.
- 621 28. Tang, P.M., Nikolic-Paterson, D.J., and Lan, H.Y. (2019). Macrophages: versatile players in
622 renal inflammation and fibrosis. *Nat Rev Nephrol* 15, 144-158.
- 623 29. Han, H.I., Skvarca, L.B., Espiritu, E.B., Davidson, A.J., and Hukriede, N.A. (2019). The
624 role of macrophages during acute kidney injury: destruction and repair. *Pediatr Nephrol* 34,
625 561-569.
- 626 30. Huen, S.C., and Cantley, L.G. (2017). Macrophages in Renal Injury and Repair. *Annu Rev*
627 *Physiol* 79, 449-469.
- 628 31. Meng, X., Jin, J., and Lan, H.Y. (2022). Driving role of macrophages in transition from
629 acute kidney injury to chronic kidney disease. *Chin Med J (Engl)* 135, 757-766.

630 32. Wei, Q., and Dong, Z. (2012). Mouse model of ischemic acute kidney injury: technical notes
631 and tricks. *Am J Physiol Renal Physiol* 303, F1487-F1494.

632 FIGURE LEGENDS

633 **Figure 1. PSMP is highly expressed in patients and mice with AKI.**

634 (A) Representative immunohistochemical staining of PSMP in normal and AKI patient kidneys.
635 Scale bars, 20 μm . (B) Statistical analysis of PSMP expression levels in normal kidneys and AKI
636 patient kidneys (NC, $n = 9$; AKI, $n = 34$). (C) Urine PSMP levels were measured by ELISA in HC
637 ($n = 8$) and AKI patients ($n = 21$) and were corrected for creatinine. (D) Plasma PSMP levels were
638 measured by ELISA in HC ($n = 36$) and AKI patients ($n = 36$). (E) Correlation analysis of urine
639 KIM-1 and PSMP levels in AKI patients ($n = 16$). (F) Correlation analysis of kidney PSMP levels
640 and the urine PSMP/creatinine in AKI patients ($n = 21$). (G) Correlation analysis of kidney PSMP
641 and plasma PSMP levels in AKI patients ($n = 34$). (H and I) Representative immunohistochemical
642 staining of PSMP in the kidney in uIRI-induced AKI and the statistical analysis ($n = 3$). Scale bars,
643 50 μm . (J) Representative immunofluorescence images of PSMP (red) and TUNEL (green)
644 staining in uIRI-induced AKI. Scale bars, 20 μm . (K) Representative immunofluorescence images
645 of LTL (green) and PSMP (red) in uIRI-induced AKI. Scale bars, 20 μm . The data are presented
646 as the mean \pm SEM. Statistical significance was determined by the Student's *t* test (B-D), Pearson
647 correlation analysis (E-G), and one-way ANOVA (I). * $P < 0.05$; ** $P < 0.01$; **** $P < 0.0001$. NC,
648 normal control; HC, healthy control.

649 **Figure 2. PSMP deficiency inhibits bIRI-induced AKI in mice.**

650 (A) Serum creatinine and BUN were measured. (B) Renal mRNA expression levels of the tubular
651 damage markers *Ngal* and *Kim-1* were measured by qPCR. (C) Representative histologic images
652 of kidney sections stained with PAS, and tubular injury score. (D) NGAL protein expression in the

653 kidney was determined by immunohistochemical staining and statistical analysis. (E) NGAL
654 protein expression in the kidney was determined by western blotting and statistical analysis ($n =$
655 3). (F) The expression of renal proinflammatory cytokine genes, including *Ccl2*, *Il-1 β* , *Il-6*, and
656 *Tnf- α* , was measured by qPCR. (G) *Ccr2* mRNA expression in the kidney was measured by qPCR.
657 Scale bars, 50 μm . $n = 5$ for each group. The data are presented as the mean \pm SEM. Statistical
658 significance was determined by two-way ANOVA. ** $P < 0.01$; *** $P < 0.001$; **** $P < 0.0001$.

659 **Figure 3. Effect of AAV9 vector-mediated hPSMP overexpression on bIRI-induced AKI in**
660 **mice.**

661 (A) The expression of hPSMP and NGAL in the kidney was measured by western blotting and
662 statistical analysis ($n = 3$). (B) Serum creatinine and BUN were measured. (C) Renal mRNA
663 expression levels of the tubular damage markers *Ngal* and *Kim-1* were measured by qPCR. (D)
664 Representative histologic images of kidney sections stained with PAS. (E) NGAL protein
665 expression in the kidney was determined by immunohistochemical staining. (F) The expression of
666 renal proinflammatory cytokine genes, including *Ccl2*, *Il-1 β* , *Il-6*, and *Tnf- α* , was measured by
667 qPCR. (G) *Ccr2* mRNA expression in the kidney was measured by qPCR. Scale bars, 50 μm . $n =$
668 5 for each group. The data are presented as the mean \pm SEM. Statistical significance was
669 determined by Tukey's multiple comparisons test. * $P < 0.05$; ** $P < 0.01$; *** $P < 0.001$.

670 **Figure 4. The PSMP-neutralizing antibody alleviates kidney injury in a bIRI mouse model.**

671 (A) Serum creatinine and BUN were measured. (B) Renal mRNA expression levels of the tubular
672 damage markers *Ngal* and *Kim-1* were measured by qPCR. (C) Representative histologic images
673 of kidney sections stained with PAS, and tubular injury score. (D) NGAL protein expression in the
674 kidney was determined by immunohistochemical staining and statistical analysis. (E) NGAL
675 protein expression in the kidney was determined by western blotting and statistical analysis ($n =$

676 3). (F) Renal mRNA levels of *Ccl2*, *Il-1 β* , *Il-6*, and *Tnf- α* was measured by qPCR. (G) *Ccr2* mRNA
 677 expression in the kidney was measured by qPCR. Scale bars, 50 μ m. $n = 5$ for each group. The
 678 data are presented as the mean \pm SEM. Statistical significance was determined by Dunnett's
 679 multiple comparisons test. * $P < 0.05$; ** $P < 0.01$; *** $P < 0.001$; **** $P < 0.0001$.

680 **Figure 5. Characteristics of Ly6C^{hi} IMs or F4/80^{lo} macrophages in uIRI-AKI mice.**

681 (A) UMAP plot colored by macrophages clusters showing the kidney macrophages annotation. (B)
 682 UMAP plot showing macrophage ontogeny (Ly6C^{hi} IMs, Ly6C^{lo} IMs, and KRM) in kidney
 683 macrophage. C6-C9 are Ly6C^{hi} IMs. (C) UMAP plot showing macrophage origin (kidney origin,
 684 blood origin and spleen origin) in kidney macrophage. C6-C9 are blood origin. (D) UMAP plot
 685 showing F4/80^{hi} macrophages and F4/80^{lo} macrophages classification in kidney macrophage. C6-
 686 C9 are F4/80^{lo} macrophages. (E) Dot plot showing *Ccr2* expression in kidney Ly6C^{hi} IMs, Ly6C^{lo}
 687 IMs, and KRM. (F) Dot plot showing *Ccr2* expression in kidney F4/80^{hi} macrophages and F4/80^{lo}
 688 macrophages. (G) Dot plot showing the scores of inflammatory cytokine, chemokine, and
 689 chemokine receptor in Ly6C^{hi} IMs, Ly6C^{lo} IMs, and KRM. (H) Dot plot showing the scores of
 690 inflammatory cytokine, chemokine, and chemokine receptor in F4/80^{hi} macrophages and F4/80^{lo}
 691 macrophages. UMAP, uniform manifold approximation and projection; KRM, kidney resident
 692 macrophages; IMs, infiltrated macrophages; hi, high; lo, low; M ϕ , macrophage.

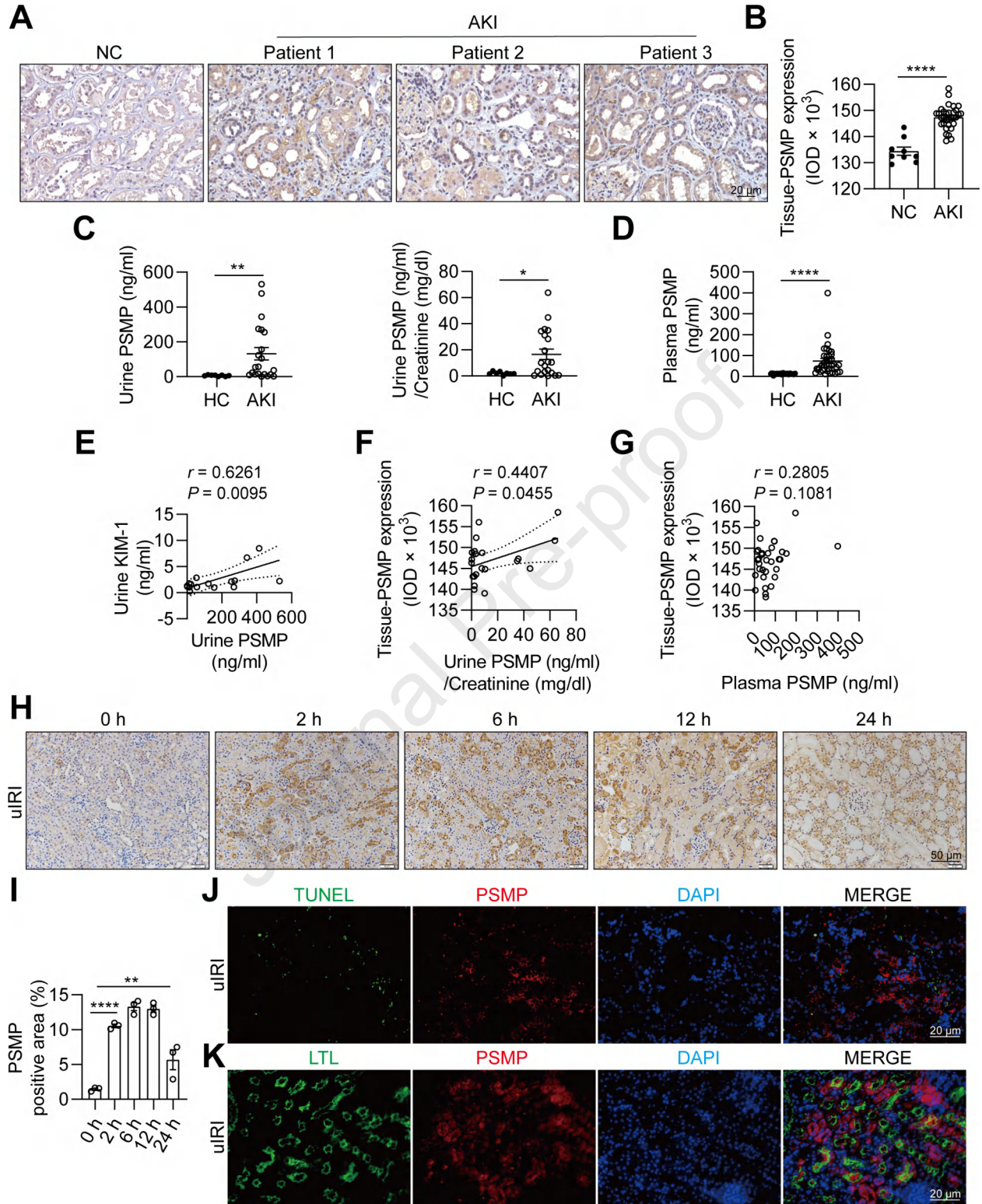
693 **Figure 6. Effects of PSMP on macrophage infiltration in bIRI-induced AKI.**

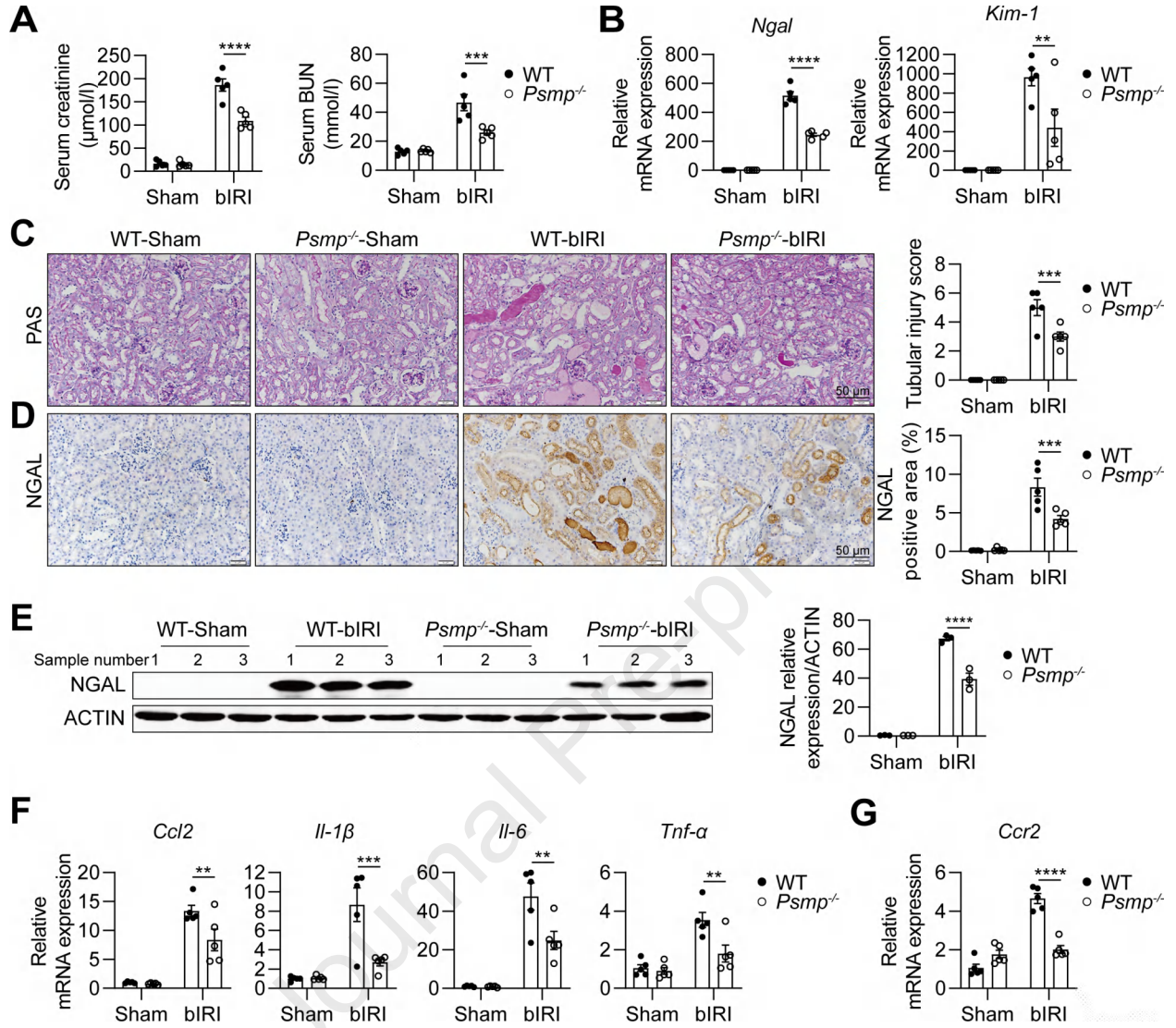
694 (A and B) Renal CD11b^{hi}Ly6C^{hi} IMs (CD45⁺Ly6G⁻) were quantified by flow cytometry. (C and
 695 D) Renal CCR2⁺Ly6C^{hi} IMs (CD45⁺Ly6G⁻) were quantified by flow cytometry. (E and F) Renal
 696 CD11b^{hi}F4/80^{lo} IMs (CD45⁺Ly6G⁻) and CD11b^{lo}F4/80^{hi} KRM (CD45⁺Ly6G⁻) were quantified by
 697 flow cytometry. $n = 5$ for each group. The data are presented as the mean \pm SEM. Statistical

698 significance was determined by two-way ANOVA. *** $P < 0.001$; **** $P < 0.0001$. IMs, infiltrated
699 macrophages; KRM, kidney resident macrophages; hi, high; lo, low.

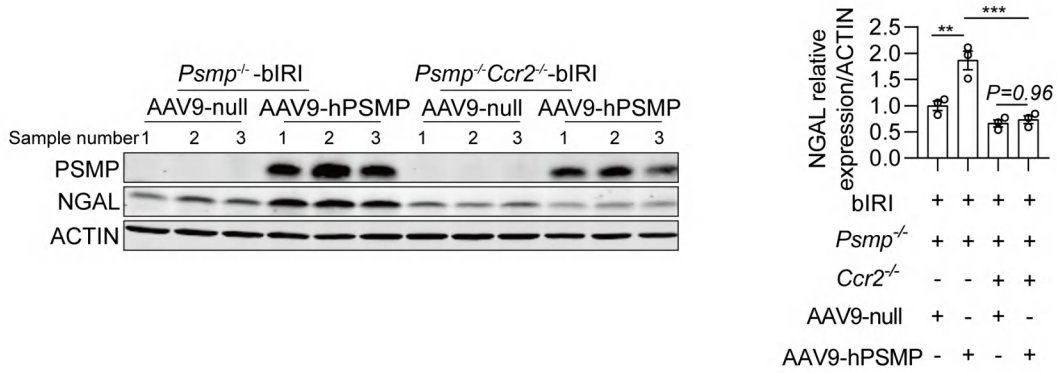
700 **Figure 7. Effects of PSMP on macrophage polarization in AKI.**

701 (A) Representative flow cytometry image of renal $CD11b^+F4/80^+$ macrophages. (B) M1 (MHCII⁺)
702 and M2 (CD206⁺) renal $CD11b^+F4/80^+$ macrophages were quantified by flow cytometry. (C)
703 Representative flow cytometric image of renal $CD11b^{hi}F4/80^{lo}$ IMs and $CD11b^{lo}F4/80^{hi}$ KRM. (D)
704 M1 (MHCII⁺) and M2 (CD206⁺) macrophages in renal $CD11b^{hi}F4/80^{lo}$ IMs were quantified by
705 flow cytometry. (E) M1 (MHCII⁺) and M2 (CD206⁺) macrophages in $CD11b^{lo}F4/80^{hi}$ KRM were
706 quantified by flow cytometry. (F) Renal mRNA expression levels of the M1 marker genes *Cd86*,
707 *Nos2*, and *Il-12* were measured by qPCR. $n = 5$ for each group. The data are presented as the mean
708 \pm SEM. Statistical significance was determined by Student's *t* test (B, D and E) and two-way
709 ANOVA (F). * $P < 0.05$; ** $P < 0.01$; *** $P < 0.001$; **** $P < 0.0001$.

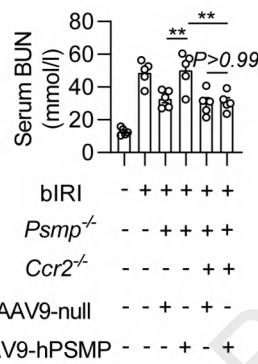
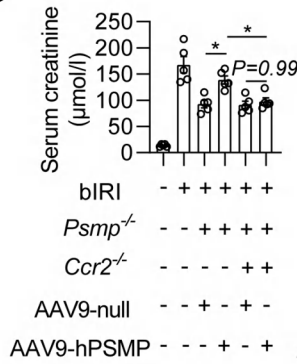




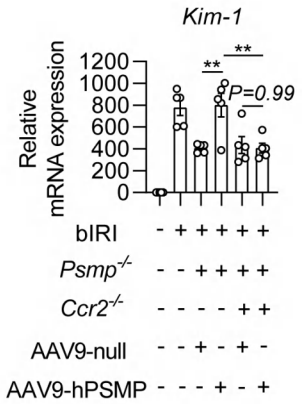
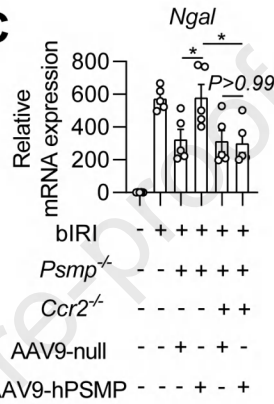
A



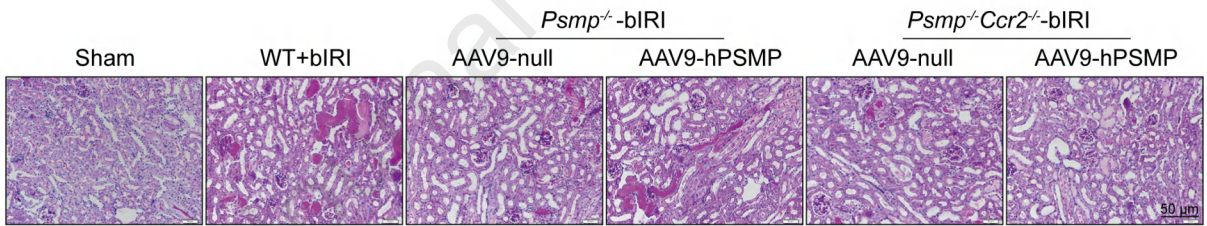
B



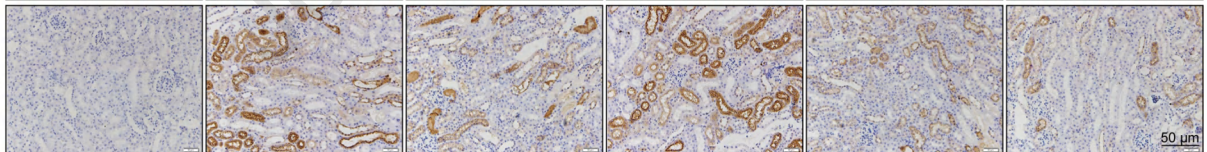
C



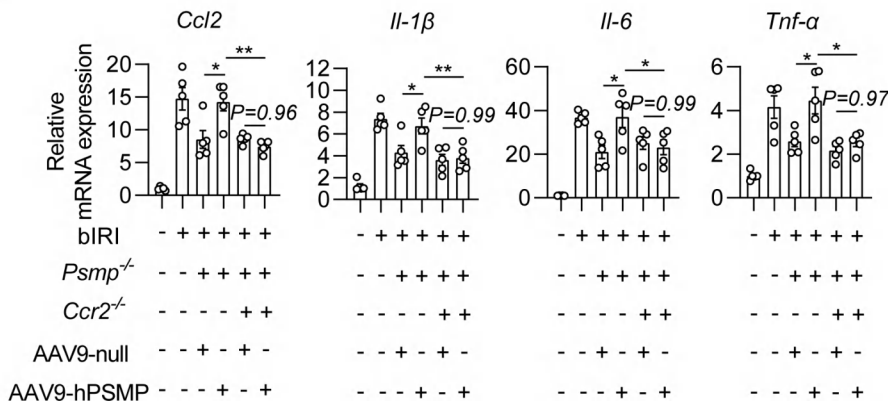
D



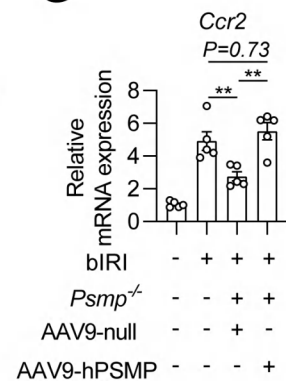
E

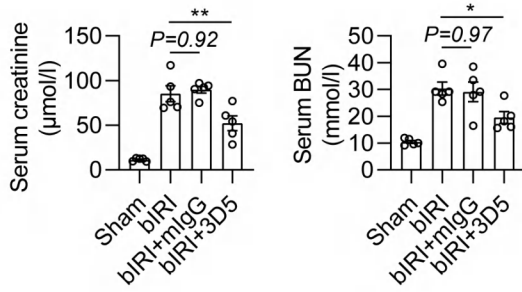
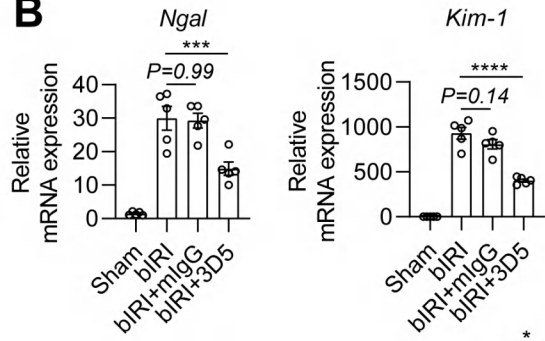
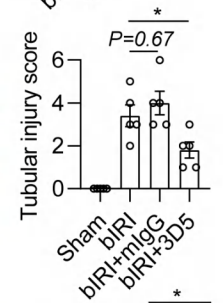
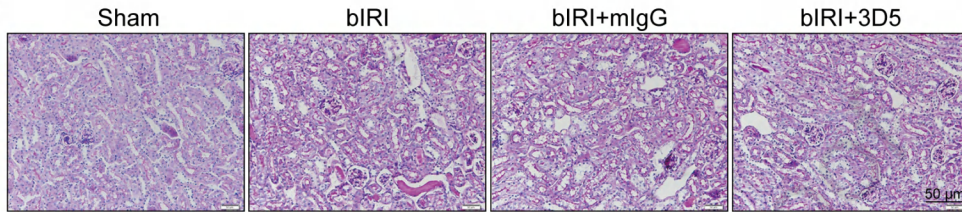
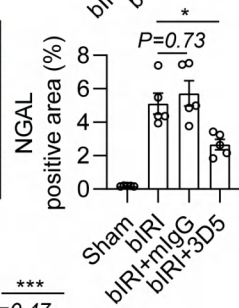
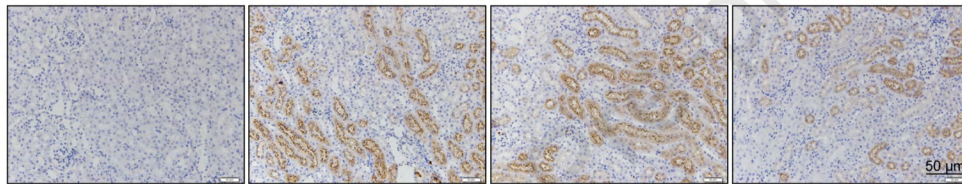
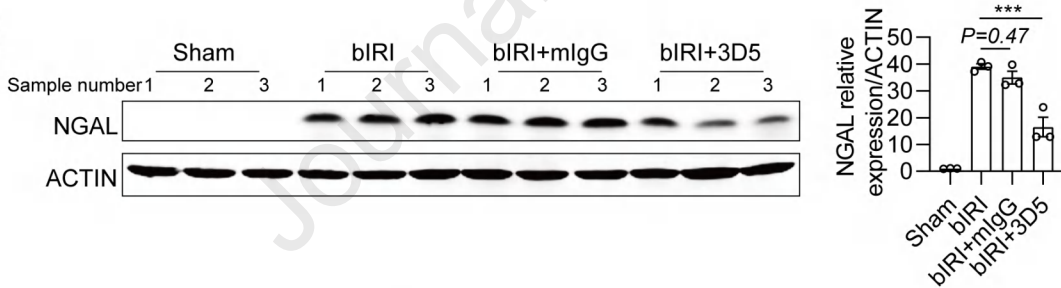
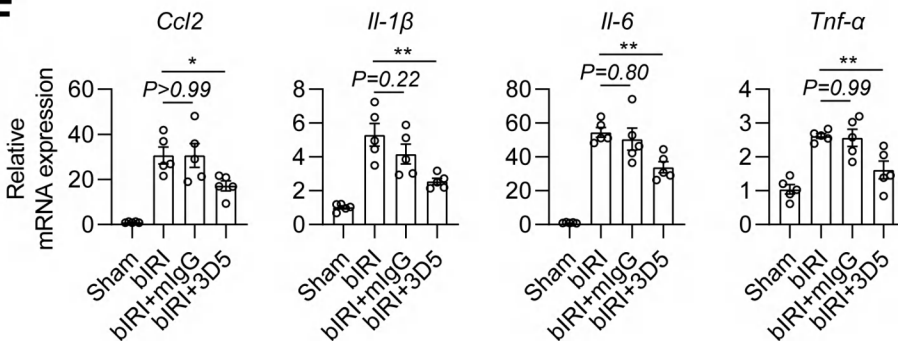
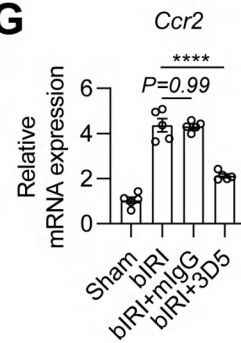


F

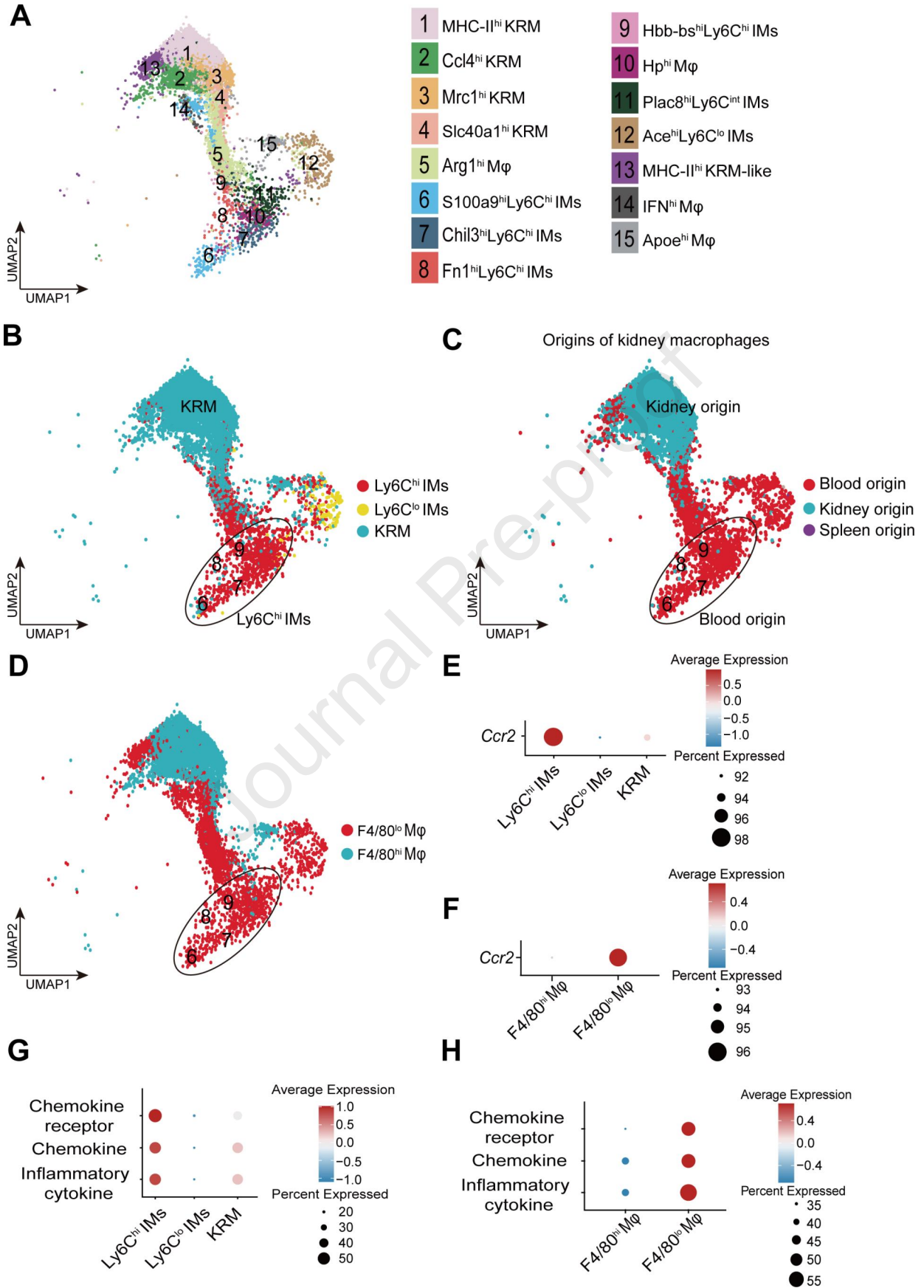


G

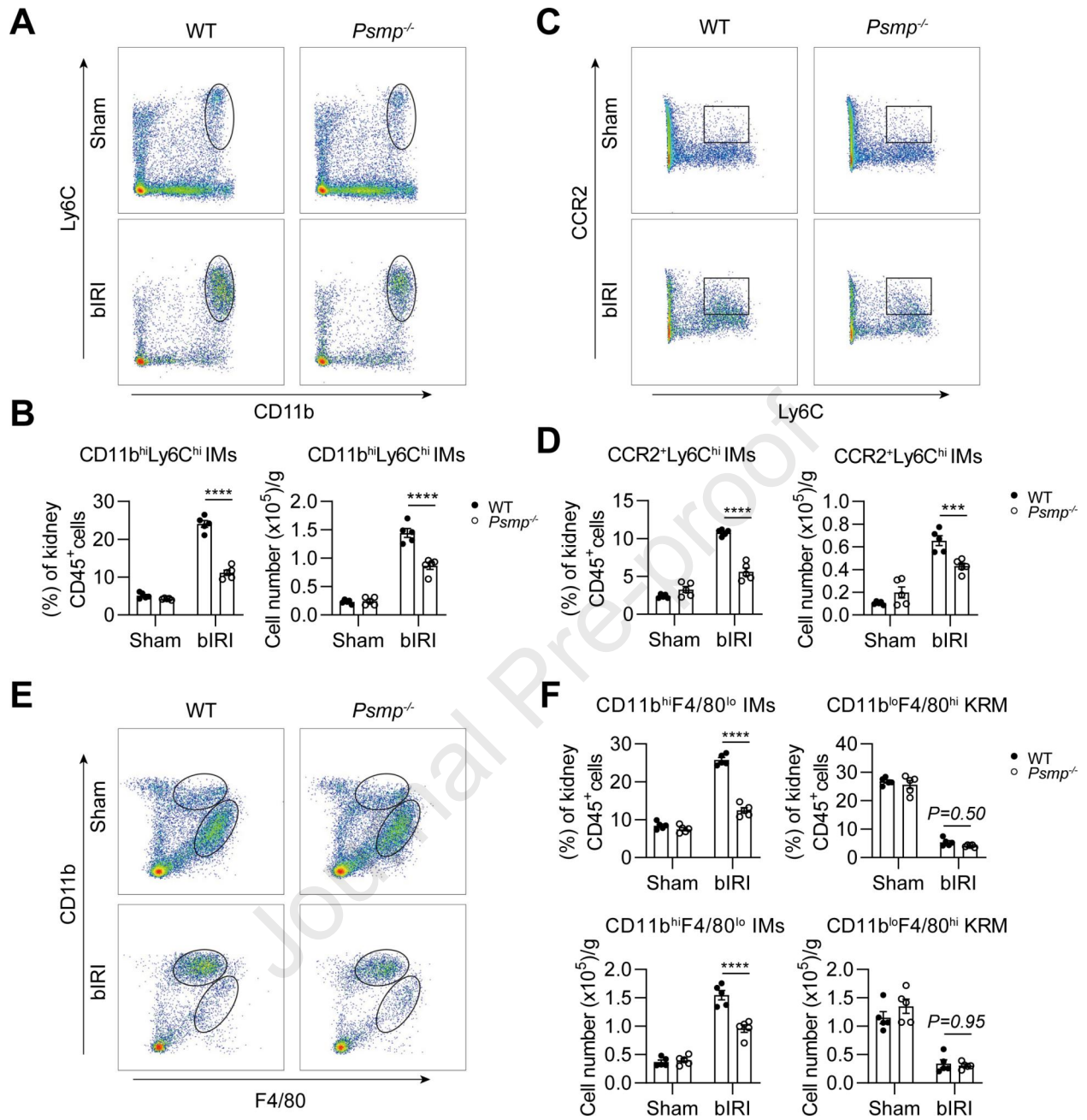


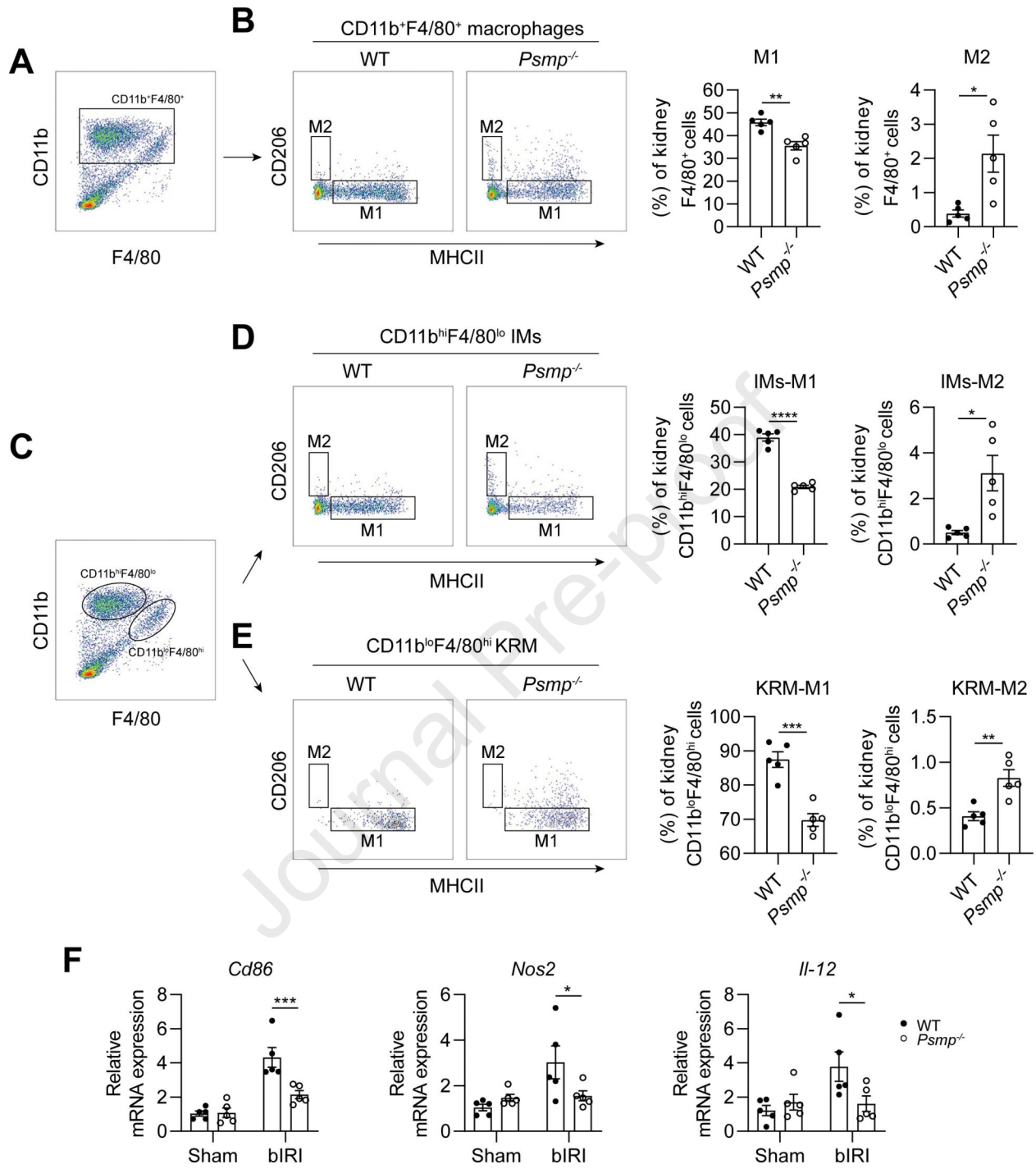
A**B****C****D****E****F****G**

Journal Pre-proof



Journal Pre-proof





Wang, Yang and colleagues reveal that PSMP, a damage-induced chemotactic cytokine, is upregulated in patients with AKI and promotes AKI in mice through CCR2-dependent inflammation. PSMP deficiency and treatment with the PSMP-neutralizing antibody 3D5 significantly alleviate AKI in mice, suggesting that PSMP is a promising therapeutic target for AKI.

Journal Pre-proof